Generalized Langevin equation approach for the rotational relaxation of a molecule trapped in a 3D crystal. II. Application to CO and CH_3F in argon

V. Delgado, J. Breton, and A. Hardisson
Departamento de Fisica Molecular, Universidad de La Laguna, Tenerife, Spain

C. Girardet[a)]
Laboratoire de Physique Moléculaire, UA CNRS 772, Université de Besançon, 25030 Besançon Cedex, France

(Received 14 January 1987; accepted 5 June 1987)

A numerical integration of the Langevin equations connected to the motions of a diatomic molecule trapped in a rare gas matrix is performed using a Runge–Kutta procedure and a Monte Carlo–Metropolis sampling for the initial configurations of the so-called primary system (cf. paper I). The rotational energy transfer from the molecule to the crystal is shown to strongly depend on the coupling between the molecule and the nearest-neighbor (NN) atoms and also on the ability for these NN atoms to dissipate their energy into the bath. Several cases are discussed according to the values of the viscous terms describing the damping of the molecule rotation and translation and of the NN atom vibrations. The prolate CH_3F molecule trapped in an argon matrix seems to relax more quickly its rotational energy than the nearly isotropic CO molecule. Special trajectory calculations, when the molecule is rotationally excited or in thermal equilibrium, are considered in order to study the well jump and the librational motion of the CO molecule.

I. INTRODUCTION

In paper I,[1] we have obtained generalized Langevin equations for the dynamics of a diatomic molecule trapped in a crystal. The orientational energy relaxation of the molecule has been interpreted in terms of viscous terms connecting the primary system, formed by the molecule rotation and translation and a limited number of nearest-neighbor (NN) atoms (j atoms), and the bath, formed by the remaining atoms of the 3D matrix. More specifically, three damping terms, which characterize the direct couplings of the rotation and of the molecule translation with the bath and the indirect coupling with the bath through the j atoms, have been analyzed in order to compare the most efficient relaxation channels.

Due to the increasing complexity of strictly 3D models, we have shown that, thanks to slight simplifying assumptions, it was possible to modify the general 3D system into an effective 2D dynamical primary system coupled to a 3D bath. The present model is then particularly well adapted to molecules with sufficiently high rotational moments of inertia and constrained to rotate in a given symmetry plane of a low temperature crystal. Such a situation seems to occur for CO trapped in rare gas crystals since several papers[2–6] have been devoted to the computation of the interaction energy and of the dynamics of this molecule as well in a quantum approach as in a classical one. Among the most recent theoretical models, Manz[4] has given a qualitative, but very interesting, description of the nature of the orientational motion of the CO molecule through the pseudorotating cage model. A somewhat similar approach has been considered by Mauricio *et al.*[6] within a strictly 2D description of the libration of the molecule strongly coupled to an undeformable shell of matrix atoms. This undeformable shell could, however, rotate around the same center as the molecule and it was coupled to the remaining crystal (the bath) with viscous damping terms. In the last decade, a lot of theoretical quantum models have also been proposed in literature, with special emphasis on the interpretation of the vibrational relaxation of CO in rare gas matrices. Multiphonon theories and libron–phonon coupling methods have been developed in monodimensional and then tridimensional models by Allavena *et al.*[5] with the aim of interpreting the experimental results obtained by Dubost[7] on one of the first studied molecule.

A second example is also considered here, with CH_3F trapped in a rare gas matrix. Indeed, this prolate symmetric top can, in first approximation, be schematized by a diatomic molecule formed by the two entities, CH_3 and F. It thus appears as a heavy rotor with the shape of a lengthened asymmetric ellipsoid, in contrast with CO which appears as a slightly anisotropic ellipsoid. Very recent potential calculations have shown[8] that the CH_3F molecule is constrained, like CO, to rotate (librate) in a crystal plane. But this orientational motion induces an important anisotropic distortion of the neighboring matrix atoms. Such a molecule has been extensively studied in high resolution spectroscopy[9] and in fluorescence or double resonance infrared–infrared experiments.[10]

Note that the present model is inadequate for hydrogenated molecules[1] (HCl, OH, NH) because, on the one hand, they cannot be considered as classical rotors and, on the other hand, the rotational motions are clearly 3D.

The paper is built as follows: Sec. II is devoted to the improvement of the previous Langevin equations, in a form convenient for a numerical computation. Reduced quantities are therefore defined and the interaction potential

a) To whom correspondence should be addressed.

 0021-9606/87/204809-14$02.10

between all the particles forming the doped matrix is discussed. The numerical procedure is developed in Sec. III where the distorted equilibrium configuration of the molecule and of the NN matrix atoms is determined in order to get the numerical values of the forces and relaxation matrices of the equations of motions. A Runge–Kutta integration procedure of the Langevin equations is then done using a preliminary statistical Monte Carlo procedure required for the determination of the initial conditions for the primary system. The numerical results are described in Sec. IV for CO and CH_3F and these results are discussed according to the values of the viscous terms.

II. REDUCED EQUATIONS OF MOTION

A more convenient form of the generalized Langevin equations of motion for the primary system formed by the molecule and the four NN atoms is obtained[1] by defining reduced quantities. A reduced time

$$\tau = \omega t \tag{1}$$

and reduced dynamical coordinates

$$\hat{\mathbf{u}}_i = \frac{\mathbf{u}_i}{a}; \quad i = (0, j = 1,...,4) \tag{2}$$

are thus defined where ω is a typical pulsation for the lattice vibration ($\omega = 2\pi \times 10^{12}\ s^{-1}$) and a is the closest distance between matrix atoms ($a = 3.756$ Å for an argon matrix). The corresponding dynamical quantities are then written in a reduced form. The forces are given by

$$\hat{\mathbf{F}}_i = \mathbf{F}_i(\hat{\mathbf{u}}_i, \theta)/(M_i \omega^2 a)\ ,$$
$$\hat{F}_\theta = F_\theta(\hat{\mathbf{u}}_i, \theta)/(I\omega^2)\ , \tag{3}$$

where M_0 and M_i $(i \neq 0) = M$ are the masses of the molecule and of a matrix atom; the viscous terms are

$$\hat{\beta}_\epsilon = \beta_\epsilon/\omega; \quad \epsilon = u_0, \theta, u_j \tag{4}$$

and the effective square frequencies

$$\hat{\Lambda}_\epsilon(0) = \Lambda_\epsilon(0)/\omega^2\ . \tag{5}$$

The reduced random forces per mass unit are finally written as

$$\hat{\mathbf{N}}_i = \mathbf{N}_i/\omega^2 a\ ,$$
$$\hat{N}_\theta = N_\theta/\omega^2\ , \tag{6}$$

with the corresponding fluctuation–dissipation relations

$$\langle \hat{\mathbf{N}}_i(0)\hat{\mathbf{N}}_i(\tau)\rangle = kT\hat{\Lambda}_i(\tau)/(M_i a^2 \omega^4)\ ,$$
$$\langle \hat{N}_\theta(0)\hat{N}_\theta(\tau)\rangle = kT\hat{\Lambda}_\theta(\tau)/(I\omega^4)\ . \tag{7}$$

All the nonreduced quantities have been defined in paper I,[1] and the equations of motion turn out to be

$$\ddot{\hat{\epsilon}}(\tau) = \hat{\mathbf{F}}_\epsilon + \hat{\Lambda}_\epsilon(0)\hat{\epsilon}(\tau) - \hat{\beta}_\epsilon \dot{\hat{\epsilon}}(\tau) + \hat{\mathbf{N}}_\epsilon \tag{8}$$

for $\epsilon = u_0, \theta - \theta_0, u_j$.

The quantities defined in Eqs. (3)–(7) are calculated using an atom–atom form for the interaction energy. The 6-exp analytical form, already used in Refs. 3 and 11 for CO trapped in an argon matrix, is extended here to the CH_3F/Ar case. This potential between two atoms l and l' is written as

$$\varphi(r_{ll'}) = -A_{ll'} r_{ll'}^{-6} + B_{ll'} \exp(-\alpha_{ll'} r_{ll'})\ , \tag{9}$$

TABLE I. Potential constants and molecular parameters.

Pair	A (kJ mol^{-1} Å^6)	B$\times 10^{-5}$ (kJ mol^{-1})	α (Å^{-1})
Ar–Ar	6554	3.27	3.305
C–Ar	3379	3.12	3.493[a]
O–Ar	2737	3.28	3.706
CH_3–Ar	4369	2.02	3.234
F–Ar	2378	2.95	3.812[b]
Molecule A–B	I (g cm^2)	δ_A (Å)	δ_B (Å)
C–O	1.45×10^{-39}	0.645	0.484
CH_3–F	3.20×10^{-39}	0.815	0.645

[a] Reference 3.
[b] Reference 17; the usual combination rules have been used for the heteronuclear pairs.

where the potential parameters are given in Table I. Such a pairwise atom–atom interaction provides a direct angular dependence for the molecule orientation and even an internal dependence through the distances δ_A and δ_B between the c.m. of the molecule and its two atoms A and B (cf. Table I).

III. NUMERICAL METHOD

Two steps in the numerical procedure are successively considered. The computation of the equilibrium configuration of the doped matrix is first required to determine the lattice distortion and the transfer matrices intervening in the expressions of $\hat{\beta}_\epsilon$ and $\hat{\Lambda}_\epsilon$. Then, Eqs. (8) are solved for several initial physical conditions of the total system.

A. Equilibrium configuration

The equilibrium configuration for the primary system is determined in order to test the adequacy of our model with the general 3D calculations. Indeed, here, the bath atoms are assumed to be nearly insensitive to the molecule inclusion ($\mathbf{d}_k \cong 0$) and only the four NN atoms (j atoms) and the molecules are relaxed from the initial perfect sites. This is obviously a restrictive hypothesis with respect to other more accurate calculations,[3,8] but this simplification is expected to have minor consequences on the dynamics of the primary system since atoms belonging to the rotation plane of the molecule will *a priori* be more perturbed by the inclusion than outside atoms.

The knowledge of the equilibrium configuration of the primary system is also a necessary information to calculate the quantities $\hat{\Lambda}_\epsilon$ and $\hat{\beta}_\epsilon$ within the framework developed in Sec. III of paper I [see also Eq. (33) of paper I].

One way of computing this equilibrium would be to minimize the potential energy v of the system [Eq. (6) of paper I]. Another way consists to solve the dynamical equations (8) after introduction of minor modifications to account for the static conditions (cf. the Appendix):

(i) The displacements $\mathbf{d}_0$ and $\mathbf{d}_j$ are taken to be zero since the coordinates $\mathbf{u}_0$ and $\mathbf{u}_j$ will now play the role of $\mathbf{d}_0$ and $\mathbf{d}_j$.

(ii) The linear term $\hat{\Lambda}_\epsilon(0)\,\hat{\epsilon}$ vanishes since $\hat{\epsilon}$ will be an instantaneous position, referred to the distorted equilibrium configuration, which must give zero at equilibrium.

(iii) The random forces $\hat{N}$ are arbitrarily taken to be zero since they do not influence the equilibrium condition.

(iv) The numerical values of the viscous terms $\hat{\beta}_\epsilon$ are conveniently chosen to obtain a rapid convergence towards equilibrium; not too small to avoid oscillations around equilibrium and not too large to permit a significant drift of the atom positions towards equilibrium. Note that such a choice has only a practical reason, as the equilibrium does not depend on $\hat{\beta}_\epsilon$. (cf. the Appendix).

Equations (8) are then solved using a Runge–Kutta[11] integration procedure for the following initial configuration; the j atoms and the molecule c.m. are taken at their perfect crystal positions and the orientation of the molecular axis is taken to be, for instance, $\theta_0^1 = \pi/2$ which corresponds to an equilibrium for AB trapped in an undistorted crystal. The initial velocities $\hat{\epsilon}$ are zero. The numerical procedure then evolved according to Eqs. (8) in a theoretical infinite time range. In fact, $\tau \sim 30$ is generally sufficient to ensure a convergence, connected [item (iv)] to the choice of $\hat{\beta}_\epsilon$, towards the equilibrium.

The values of $\hat{\epsilon}$ thus obtained correspond to the equilibrium positions $\mathbf{d}_0$, d_j, and θ_0 which are given in Table II for CO and CH_3F trapped in an argon lattice. For comparison, we also give the distortion vectors obtained from direct minimization of the potential energy of the 3D doped crystal.[3,8] Our results for the four atoms and the molecule satisfactorily agree with accurate 3D calculations for CO; the agreement is not as good for CH_3F. These results are not surprising in the sense that the symmetric top molecule has a larger anisotropic size than CO. The accurate calculations account for a distortion over four matrix shells (56 atoms, instead of 4 here!) for CH_3F. Moreover, the C_3 symmetry of the molecule is taken into account in the accurate calculations while CH_3F is regarded here as a diatomic molecule. The energy gain due to the matrix distortion with respect to the undistorted configuration exhibits the same discrepancy for the same reason. Note, however, that the values of the molecule position and orientation issued from the two types of calculations are very close.

The fact that our results are not too different from other statical calculations may be considered as a promising feature. Indeed, this means that the computation of the dynamics of the primary system rests on a convenient 3D statical basis. Accuracy would lead to use of the 3D results, but consistency requires that we take our results for the study of the dynamics!

B. Determination of the matrices $\hat{\Lambda}_\epsilon$ and $\hat{\beta}_\epsilon$

These general 3D matrices are in fact reduced to 2D for the vibrations of the primary system and to 1D for the molecule orientation. They are matrices obtained as a sum of the square of matrices of which the elements are force constants connecting the atoms of the crystal. The sum over the atoms is rapidly convergent when these atoms are inside a sphere of radius $3a$ for each j atom or for the molecule. The matrices can be expressed in terms of a single matrix $\hat{T}$ as

$$\hat{\beta}_\epsilon = (\Gamma/\omega)\hat{T}_\epsilon\,,$$
$$\hat{\Lambda}_\epsilon(0) = (\Omega/\omega^2)\hat{T}_\epsilon\,, \qquad (10)$$

where $\hat{T}_\epsilon$ depends on the second derivatives of the interaction potential and has a definite value for a given potential. In contrast, Γ/ω and Ω/ω^2 will be free to vary in the following. We give, in Table III, the nonzero elements of $\hat{T}$.

The matrix $\hat{T}_j$ characterizes the jth atom; its diagonal terms are nearly the same and they have been taken to be strictly equal and normalized to unity; the nondiagonal elements remain small and they would vanish exactly if the j atom "saw" an isotropic crystal (i.e., in the absence of the molecule and of the concomitant lattice distortion). Note that the nondiagonal elements of $\hat{T}_j$ can be larger for CH_3F than for CO as expected by the larger anisotropy of the symmetric top.

The matrix $\hat{T}_0$, connected to the molecule, is diagonal

TABLE II. Distortion of the primary system.

	CO		CH_3F	
Molecule	This work	Reference[a]	This work	Reference[b]
d_{1X}(Å)	0.031	0.031	0.054	0.026
d_{1Z}	0.047	0.026	0.066	0.020
d_{2X}	0.031	0.031	0.054	0.025
d_{2Z}	−0.047	−0.026	−0.066	−0.022
d_{3X}	−0.034	−0.030	−0.060	−0.039
d_{3Z}	−0.063	−0.029	−0.120	−0.064
d_{4X}	−0.034	−0.030	−0.060	−0.043
d_{4Z}	0.063	0.029	0.120	0.067
d_{0X}	−0.275	−0.249	−0.571	−0.530
d_{0Z}	0	0	0	0
θ_0	$\pi/2$	$\pi/2$	$\pi/2$	$\pi/2$
E (cm^{-1})[c]	−68	−127	−309	−520

[a] See Ref. 3 for a 3D relaxation of the crystal.
[b] See Ref. 8 for a 3D relaxation of the crystal and including four shell relaxations.
[c] Energy gain by matrix relaxation.

TABLE III. Numerical data for the matrices $\hat{T}_\epsilon$.[a]

		XX	ZZ	XZ
$\hat{T}_1$	CO	1	1	−0.072
	CH_3F	1	1	0.006
$\hat{T}_2$	CO	1	1	0.072
	CH_3F	1	1	−0.006
$\hat{T}_3$	CO	1	1	−0.041
	CH_3F	1	1	0.118
$\hat{T}_4$	CO	1	1	0.041
	CH_3F	1	1	−0.118
$\hat{T}_0$	CO	0.908	0.183	0
	CH_3F	0.916	0.267	0
$\hat{T}_\theta$	CO	0.275	...	...
	CH_3F	0.682	...	...

[a] These results are for $\gamma = 1$; for $\gamma = 2, 3, 4$, corresponding equivalent results can be obtained after applying the symmetry rules of the crystal.

since the molecule site is the only site from which one can see a nearly isotropic crystal if we expect the distortion. The larger the molecule anisotropy is, the more different the diagonal elements are. The $(1\times1)\hat{T}_\theta$ matrix is larger for CH_3F than for CO and generally remains smaller than the diagonal terms of $\hat{T}_j$ and $\hat{T}_0$. We can thus expect, from this feature, a more efficient energy transfer from the vibrational motions than from the orientational one.

At this stage, all the quantities appearing in Eqs. (8) are known, and we can then solve these dynamical equations where the temperature is introduced through the fluctuation–dissipation theorem [Eqs. (7)].

C. Dynamical computations

The numerical integration of Eqs. (8) is done using a Runge–Kutta procedure after a Monte Carlo–Metropolis sampling for the initial configurations. The development of the statistical method has been extensively explained in Ref. 12 and we give here the specificity of the method when applied to our case.

An initial configuration P for the primary system is chosen to be the distorted equilibrium configuration for the positions $\hat{\epsilon}$, $(\mathbf{d}_0,\mathbf{d}_j,\theta_0)$, and the following thermal velocities for each component of $\dot{\hat{\epsilon}}$:

$$\dot{\hat{\epsilon}} = \pm (kT/2M_\epsilon)^{1/2}, \tag{11}$$

where the sign is randomly assessed. A numerical integration of Eqs. (8) is then performed with $\hat{\beta}_\epsilon = \hat{\Lambda}_\epsilon(0) = 0$ for $\tau\sim30$ in order to obtain a better configuration P_0. Within this model, the bath does not influence the primary system and the temperature is fixed at its value T.

The Monte Carlo sampling is then applied from this configuration P_0 as described in Ref. 12. The positions and the velocities of the atoms and of the molecule belonging to the primary systems are then moved in succession using a random generator. A new configuration is accepted each time that the lattice energy is lowered with respect to the previous one or, if not, each time that the Boltzmann probability ratio for this configuration with respect to the previous one is greater than a random number in the range (0,1). A sampling of about 6×10^4 random walks has been performed at this first stage. Such a procedure allows us to improve the convergence, i.e., to obtain a final configuration P_1 which is expected to be more probable for the system than the previous configuration.

This latter accepted configuration P_1 is considered to be the new initial configuration for the integration of the Langevin equations and the determination of the various observables of the primary system: kinetic, potential, and mechanical energies and autocorrelation functions of the molecular axis.

Then a sequence of r random configurations starting from the initial configuration P_1 is constructed before another numerical integration of the Langevin equations is achieved. This procedure is repeated p times, then the sequence length is changed into $50r$ before a new integration and a new sequence of r random walks. r and p have been varied within the ranges [10,30] and [6,10], respectively. The convergence is obtained for 800 to 1600 trajectories according to the molecule and to the physical conditions, and the mean values of the observables have then been calculated.

Note still that the numerical procedure must be modified to introduce particular initial conditions in the Langevin equations. Beside the general method used before, we have considered the case of an orientational excitation of the molecule with

$$\dot{\theta} = [kT^*/(2I)]^{1/2}; \quad T^* = 50T. \tag{12}$$

These data must be introduced in the different P_i $(i\geqslant1)$ configurations which have been retained to calculate the trajectories. However, the atom velocities and positions and the molecule positions are not changed with respect to the previous development.

Another case has also been considered when the molecule orientation is arbitrarily fixed at a maximum $(\theta=\pi/4)$ or at a minimum $(\theta=\pi/2)$ of the interaction energy. The Monte Carlo sampling is therefore done on the positions and velocities of the particles of the primary system.

A particular feature connected to the rotational motion of the molecule must also be mentioned. When, within a given trajectory, the molecular axis jumps from a given well γ to another one γ', we have to renormalize the equations of motion. This means that a new equilibrium configuration must be defined with respect to the γ' well ($\mathbf{d}_\epsilon^\gamma$ changes into $\mathbf{d}_\epsilon^{\gamma'}$) and the corresponding dynamical variables $\epsilon^{\gamma'}$, in the new well, are such that

$$\mathbf{u}_i^{\gamma'} = \mathbf{d}_i^{\gamma'} - \mathbf{d}_i^{\gamma} + \mathbf{u}_i^{\gamma}; \quad i=(0,j)\,. \tag{13}$$

Moreover, since the equilibrium configuration is changed, the primary system-bath coupling terms $\hat{\Lambda}_\epsilon$ and $\hat{\beta}_\epsilon$ must also be changed and recalculated for this new equilibrium.

The same renormalization is again used for the initial conditions as calculated by the Monte Carlo sampling. Due to the symmetry of the problem, the probability for finding the molecular axis must be the same in the four wells. The temperature values used here ($T\sim20$ K) prevent jumps from one well to another in the Monte Carlo sequences. So we have rotated the whole crystal, by fixing the axis system, by successive rotations of $\pi/2$; such a process is equivalent to force the molecular axis to jump from one well to another.

IV. RESULTS AND DISCUSSION

High resolution spectroscopy and time-resolved experiments provide two complementary species of informations regarding the phase and energy relaxations of the molecule vibration. Two physical situations are considered which can be connected directly to the influence of the orientational motions on the lifetime of the excited vibrational level of a molecule and on the linewidth of its near infrared spectrum. In the first case, the molecular rotation is assumed to be highly excited by a direct and partial transfer of the vibrational energy. This excitation is simulated by raising the equivalent rotational temperature of the molecule to $T^*=50T$, where T is the bath temperature ($T=20$ K). Note that this temperature T^* corresponds in fact to a small part of the possible excitation energy issued from the vibrational deexcitation of a CO molecule ($T^*\sim300T$) or of a

CH_3F molecule ($T^* \sim 150T$). The relaxation of the rotational energy towards the primary system and the bath is then analyzed. In the second case, the temperature of the whole doped crystal is fixed at $T = 20$ K and the trajectories of the molecule and of the atoms of the primary system are computed according to different initial configurations for the molecular axis. Moreover, the values of Γ/ω and Ω/ω^2 have been varied in order to analyze the influence of the system and bath viscosities. For each selected case, we will compute the time behavior of the averaged rotational and translational kinetic energies $\bar{K}_\theta$ and $\bar{K}_0$ of the molecule, of the mean vibrational kinetic energy $\bar{K}_A$ of the four j atoms, of the mean potential energy $\bar{V}$ of the primary system and of its total mechanical energy $\bar{E}$, and of the correlation function $\bar{F}$ of the dipolar axis of the molecule.

A. Rotational excitation $T^* = 50T$

1. CO trapped in an argon matrix

a. Theoretical damping. Figure 1 exhibits the behavior with τ of $\bar{K}_\theta$, $\bar{K}_0$, $\bar{K}_A$, $\bar{V}$, $\bar{E}$, and $\bar{F}$ for the theoretical values: $(\Gamma/\omega) = 0.16$ and $(\Omega/\omega^2) = 0.024$. Three steps can be distinguished in the relaxation mechanism:

$0 < \tau \lesssim 2$ corresponds to the transient regime. The main part of the rotational energy is dissipated towards the kinetic energy of the molecule c.m. and of the j atoms and also transformed into potential energy. The primary system relaxes about 30% of $\bar{K}_\theta$ into the bath directly through the molecule rotation or, indirectly, through the j atoms.

$2 \lesssim \tau \lesssim 6$ corresponds to an enlarged transient–stationary regime for the primary system. The energy excess is located mainly on the c.m. vibrations of the particles of the primary system with a possible feedback transfer from the j atoms to the molecule c.m., and to the rotation in a smaller extent. The energy $\bar{E}$ of the primary system monotonously decreases.

$\tau \gtrsim 6$, corresponds to the stationary regime where the remaining energy excess is dissipated towards the bath. Figure 2 shows the various deexcitation channels with the concomitant efficiency (in energy unit) of these channels in the first stages of the time evolution. A relative equipartition of the energy seems to be observed for the various dissipation channels. Note again that the correlation function $\bar{F}$ monotonously decreases and is zero after about ten oscillations of the bath atoms.

b. Increasing damping. When the viscous term Γ/ω is twice larger ($\Gamma/\omega = 0.32$) the overall time behavior of the computed observables for $\Gamma/\omega = 0.16$ is quite similar, but

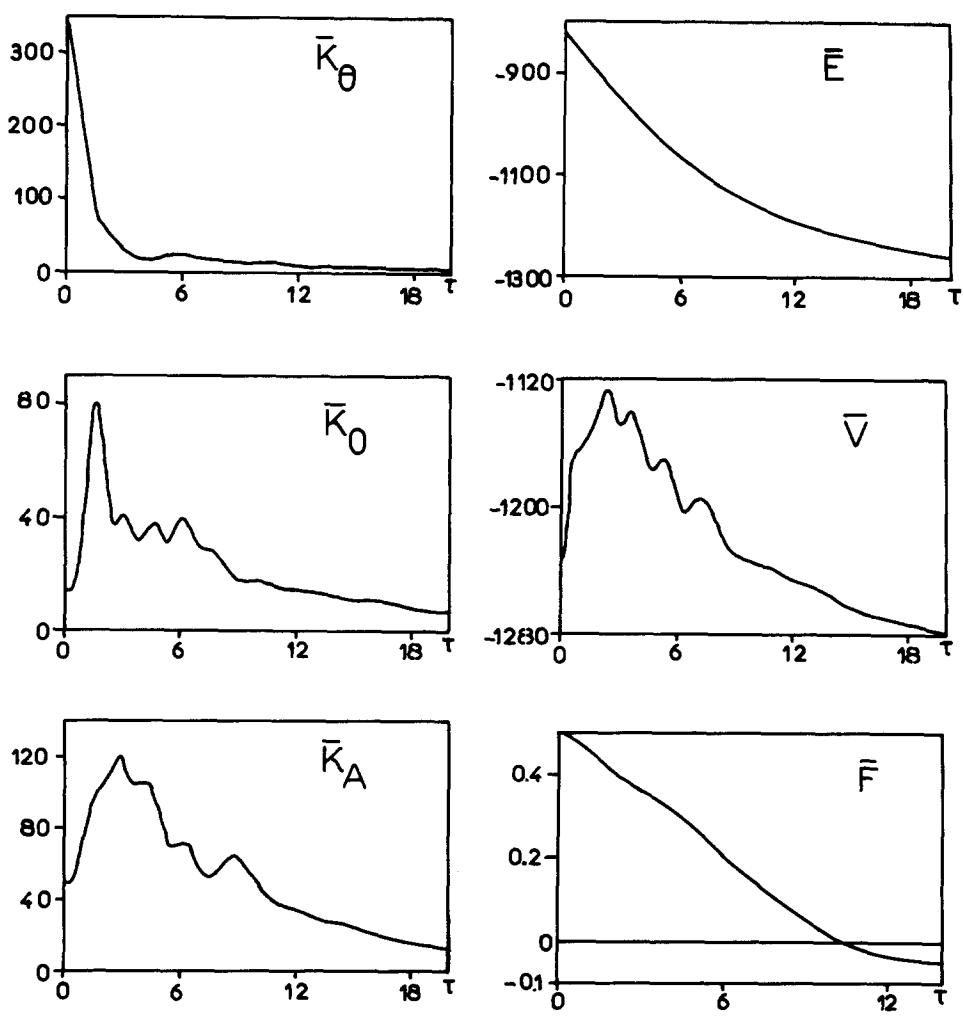

FIG. 1. Time behavior of the observables of the primary system formed by a CO molecule and four Ar atoms $\Gamma/\omega = 0.16$ and $\Omega/\omega^2 = 0.024$, $T = 20$ K, $T^* = 50T$. Left: mean rotational kinetic energy $\bar{K}_\theta$ and vibrational kinetic energies $\bar{K}_0$ and $\bar{K}_A$ for the molecule c.m. and the four atoms. Right: total energy $\bar{E}$ and potential energy $\bar{V}$ of the primary system, and autocorrelation function $\bar{F}$ for the molecular axis. All energies expressed in cm^{-1} unit and time in reduced unit.

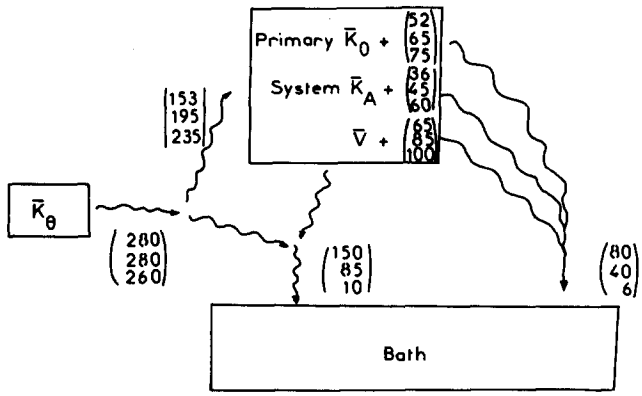

FIG. 2. Energy balance for the total system. The transfers are schematized by corrugated arrows and the corresponding magnitudes are given within brackets for $\Gamma/\omega = 0.32$ (upper value), 0.16 (middle), and 0.016 (lower), respectively.

not in the details (cf. Fig. 3). In the transient regime $\tau \lesssim 2$, the rotational energy loss is the same (~ 280 cm^{-1}), but 55% only, instead of 70% in the first case, of this energy is transferred to the remaining primary system. The bath receives from the primary system an energy twice as large because $\bar{E}$ decreases much more rapidly. This is a striking feature of the behavior of the energy relaxation when the viscosity increases. Indeed, as discussed in paper I, an increase of Γ/ω leads to an increase of the various viscous terms $\hat{\Lambda}_\theta(\tau)$, $\hat{\Lambda}_0(\tau)$, and $\hat{\Lambda}_j(\tau)$. We thus would expect an increased efficiency of the energy relaxation channels. But this relaxation seems to be unfavorable to the primary system channel, in the sense that it cannot accept energy because it is more damped by $\hat{\Lambda}_j(\tau)$. In contrast, the direct relaxation due to $\hat{\Lambda}_\theta(\tau)$ seems to be enhanced by the viscosity increase. This results from the already mentioned antagonistic effects (cf. paper I). In the intermediate regime, the features are not too different from the less damped case. The main difference is due to the damping of the j atoms which leads to a less oscillatory behavior of the kinetic and potential energies $\bar{K}_A$ and $\bar{V}$. Note also that the remaining rotational energy for $\tau > 2$ is less important in this case and that the correlation function is zero for τ around 18. Thus, we are led to conclude that, although the energy relaxation is enhanced, the correlation function is less damped. This apparent paradox can nevertheless be very well understood if we consider the antagonistic effects mentioned before. Indeed, the molecule sees the j atoms as poor energy acceptors since these atoms are relatively damped. So the collisions between

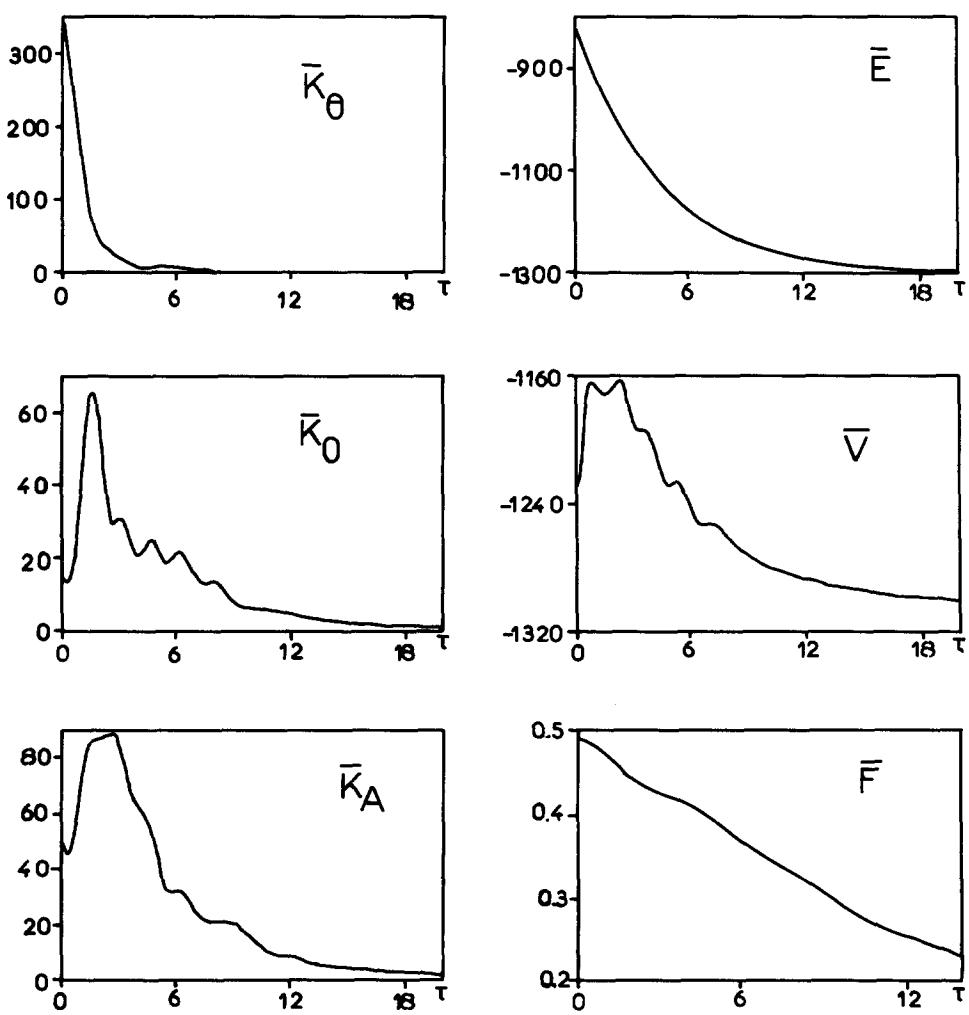

FIG. 3. Same as for Fig. 1, but for $\Gamma/\omega = 0.32$.

the molecular rotation and the vibrations of the j atoms are inefficient inelastic collisions, with an apparent consequence that the molecule is freer in this case.

This mechanism may be of the same type as that which occurs in quantum systems, due to rapid dephasing. Caldeira and Legett[13] have shown that quantum tunneling, which is generally expected to be the predominant decay mode of a metastable state, can be considerably reduced by the increase of the friction in macroscopic systems; or, in other words, that the tunneling effects are diminished by the damping from the heat bath.[14] An extensive discussion and the corresponding bibliography of the phenomena connected to this mechanism can be found in Ref. 15. Further analyses of this mechanism are left for a forthcoming paper where the vibrational relaxation of the same molecule will be studied through the vibration–rotation–lattice vibration couplings and by including effective quantum (low temperature) effects.

c. Decreasing damping. When the viscous parameter Γ/ω is ten times smaller ($\Gamma/\omega = 0.016$) than the theoretical value, the behavior of the computed observables differs in a considerable way (cf. Fig. 4).

In the transient regime $\tau \lesssim 2$, the rotational energy loss is nearly the same as for the previous cases (a) and (b) ($\sim 260\ \mathrm{cm}^{-1}$), but now the primary system takes 90% of this energy and the bath receives a negligible part of it ($< 10\ \mathrm{cm}^{-1}$), as shown by the slow decrease of the energy $\bar{E}$.

When $\tau > 2$, the vibrational motions keep this energy either in their kinetic or in their potential parts and the primary system thus appears as a self-consistent mechanical system which exchanges energy inside its own degrees of freedom, as shown by the oscillations of $\bar{K}_0$, $\bar{K}_A$, and $\bar{V}$. The bath is quite inefficient.

The autocorrelation function is strongly damped, over five oscillations of the crystal atoms, by the collisions between the molecule rotation and the primary system vibrations. Note, however, that this autocorrelation function tends to oscillate around the zero value for long τ times, whereas the rotational energy never decreases to zero, at least up to $\tau = 20$. About $40\ \mathrm{cm}^{-1}$ of the rotational energy is kept by the molecule as the result of the energy exchanges between the various motions of the primary system.

Note, finally, that a change of the effective frequencies $\hat{\Lambda}_\epsilon(0)$, through the change of the ratio (Ω/ω^2), does not

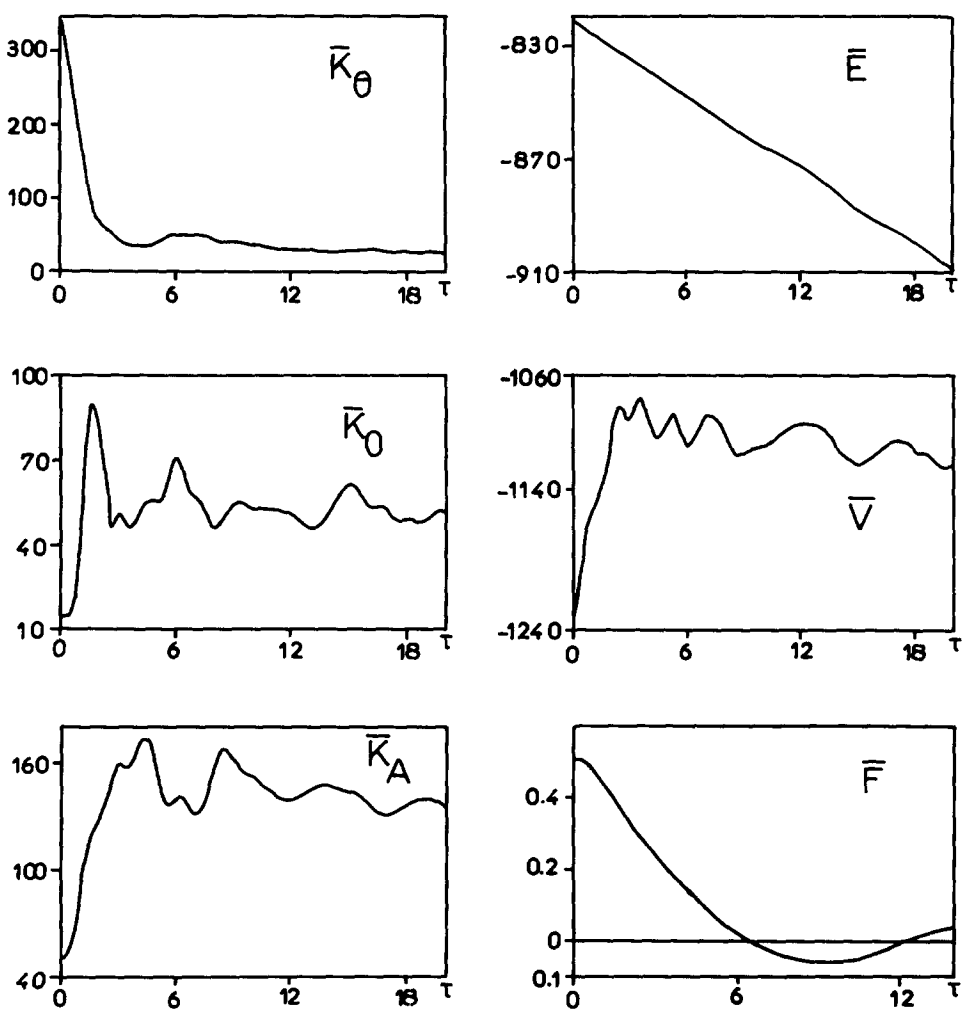

FIG. 4. Same as for Fig. 1, but for $\Gamma/\omega = 0.016$.

influence the various behaviors described here and therefore the curves connected to $(\Omega/\omega^2) = 0.24$ and 0.0024 are not given here.

2. CH_3F trapped in an argon matrix

The various observables for the CH_3F molecule, assimilated to a diatomic CH_3–F molecule, have been computed for the theoretical value of the viscous parameter $\Gamma/\omega = 0.16$. The values Γ/ω and Ω/ω^2 which depend only on the solid characteristics are the same as for CO.

The behavior of the energy relaxation still appears in a much clearer way than for CO (Fig. 5).

In the transient regime, the rotational energy relaxation ($320\ cm^{-1}$) appears more efficient than for CO. A yield of $85\ cm^{-1}$ is transferred to the molecule c.m. kinetic energy, only $50\ cm^{-1}$ are given to the kinetic energy of the four j atoms and $155\ cm^{-1}$ to the potential energy $\bar{V}$. The bath gains about $30\ cm^{-1}$. The intermediate regime (for $2 \lesssim \tau \lesssim 10$) is longer than for CO. The c.m. of the molecule and the potential energy of the primary system transfers a part of this energy ($\sim 140\ cm^{-1}$), on the one hand, to the j atoms ($\sim 50\ cm^{-1}$) and, on the other hand, to the bath ($\sim 90\ cm^{-1}$) for $\tau \sim 4$, as shown by the strong peaks observed in $\bar{K}_0$ and $\bar{K}_A$.

Beyond $\tau \sim 10$, a part of the excitation remains on the primary system with feedbacks towards the molecule rotation and translation. The decrease of the energy $\bar{E}$ of the primary system is similar to what is observed for CO. The behavior of the autocorrelation function is very different of the monotonous decrease exhibited for CO in Fig. 1. Indeed, for the same value of Γ/ω, the decrease is not so fast for CH_3F and this therefore leads to a greater relaxation time for the molecular axis.

B. Thermal conditions $T^* = T$

Three typical cases have been considered. They correspond to the normal time evolution of the primary system at thermal equilibrium and to the time evolution of the system, when the molecular axis is forced to be located at the bottom of a potential well or at the top of the energy maximum. No significant differences occur between the three cases, except for the rotational energy. Figure 6 shows the evolution of the kinetic energy when the molecular axis is located at a minimum or at a maximum of the potential well. An obvious behavior for $\bar{K}_\theta$ is observed since, when $\theta = \theta_{min}$, the kinetic energy is maximum and decreases at the expense of the potential energy when the molecule librates in its well up to a potential maximum where the kinetic energy takes a mini-

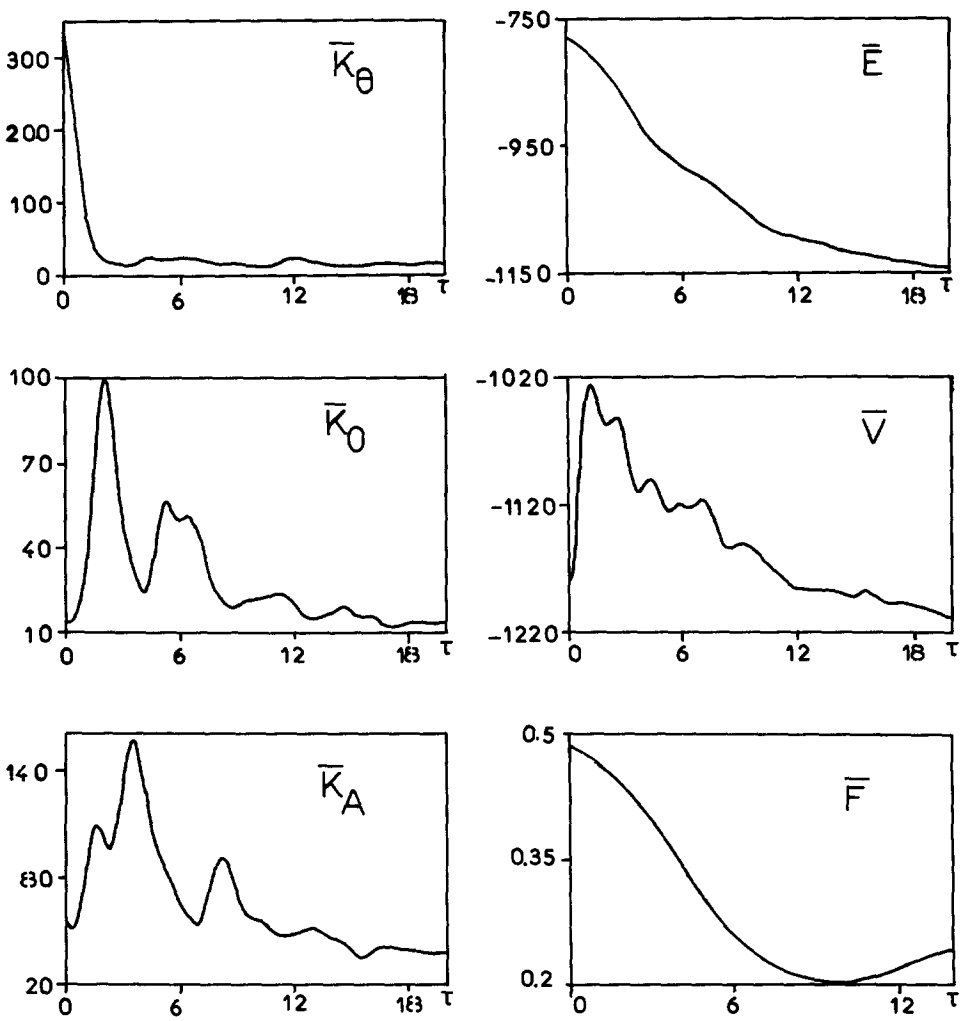

FIG. 5. Same as for Fig. 1 but for a CH_3F molecule and $\Gamma/\omega = 0.16$.

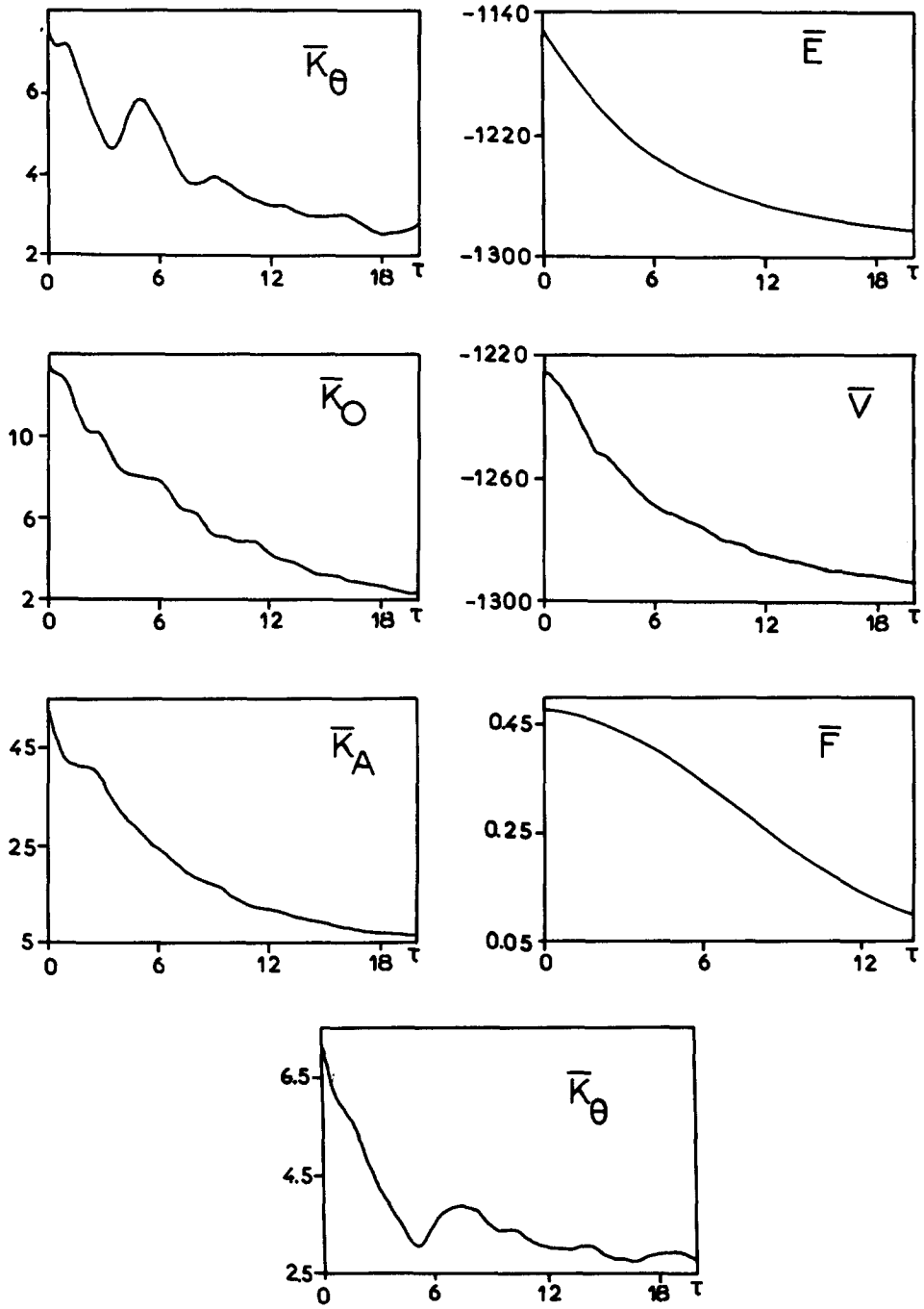

FIG. 6. Time behavior of the observables of the primary system formed by CO and four argon atoms, for the thermal conditions $T = T^* = 20$ K and $\theta = \theta_{max}$ (six upper pictures). Lower picture: $\bar{K}_\theta$ for $\theta = \theta_{min}$.

mum value and so on. When $\theta = \theta_{max}$, in contrast, the kinetic energy has its minimum value which increases up to the minimum of the well and decreases before the molecule stops and comes back. The other observables of the primary system have a regular decrease due to the damping. The autocorrelation function of the dipolar axis of CO decreases over a large time scale for the three cases, leading to a relaxation time for the molecular axis around 3 ps. The same conclusions have been reached for CH_3F with a greater relaxation time.

C. Comparison of the trajectories for CO trapped in argon

Selected trajectories for the primary system formed by a CO molecule and four argon atoms have been computed, in a separate way, with the theoretical conditions $\Gamma/\omega = 0.16$ and $\Omega/\omega^2 = 0.024$. Two types of trajectories are discussed here according to the molecular rotation which is excited ($T^* = 50T$) or not ($T^* = T = 20$ K).

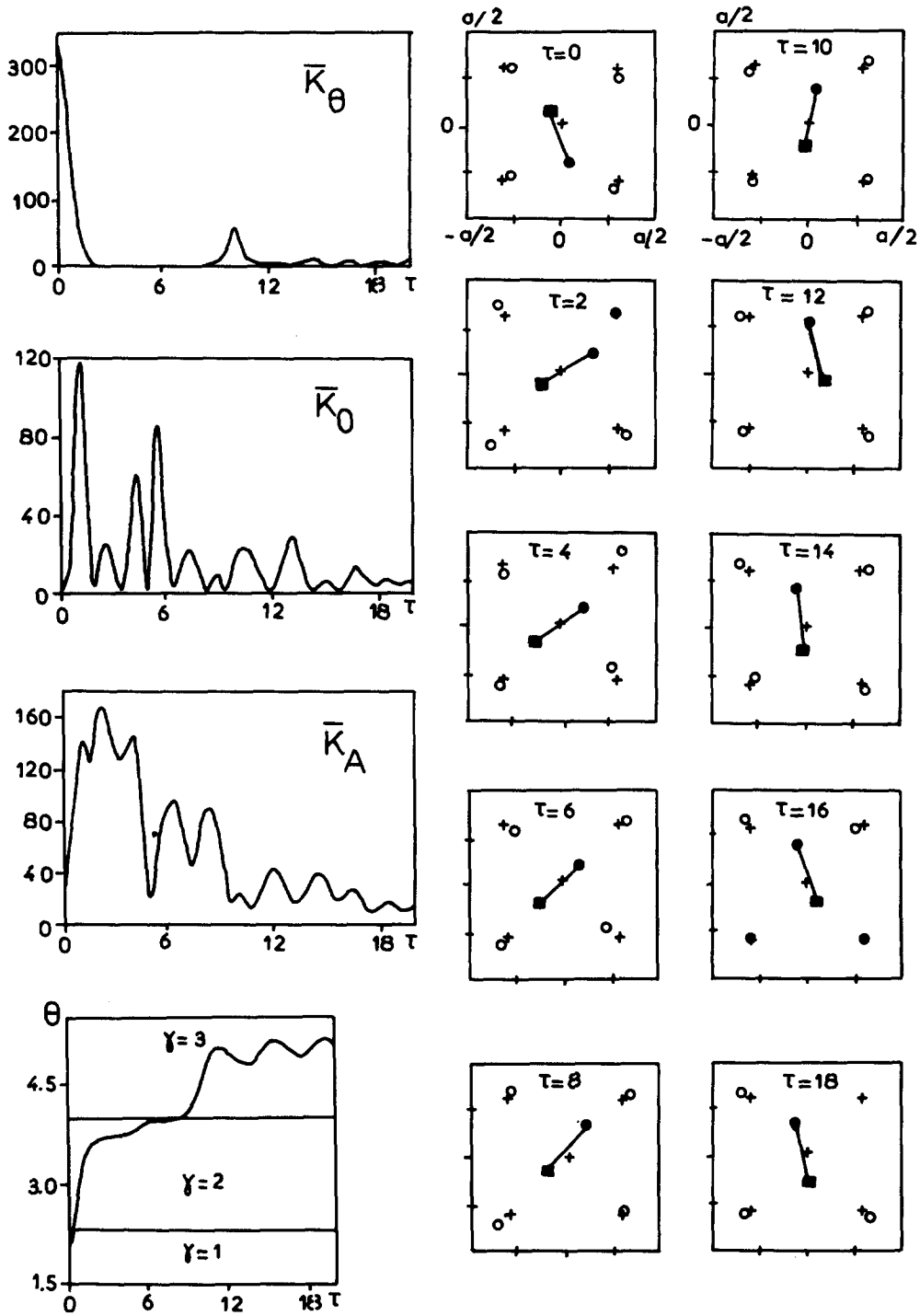

FIG. 7. Kinetic energies of the primary system (CO + four Ar) for a particular trajectory and for $\Gamma/\omega = 0.16$, $\Omega/\omega^2 = 0.024$, and $T^* = 50T$, $T = 20$ K; time behavior of the angle θ and photographs of various instantaneous configurations for the primary system. The + corresponds to the perfect crystal site and ● to the instantaneous positions of the c.m. The molecule CO is pictured by ×—■ (× for C and ■ for O). All energies are in cm^{-1} unit. The displacements of the atom and of the molecule are expressed in Å; $a = 3.756$ Å is the measure of the side of each square. Note that the distance between the crystal sites is not at scale.

1. Rotational excitation

Figure 7 exhibits the behavior with time of the kinetic energies of the molecular rotation and translation and of the four j atoms when the equations of motions are integrated at the P_1 configuration. Note that these curves show oscillations for large τ values and that the molecular rotation can gain energy around $\tau = 10$. This gain corresponds to the increase of the rotational velocity after the molecule has gone through a potential maximum. In fact, the molecular axis investigates three consecutive wells ($\gamma = 1$, 2, and 3).

At $\tau = 0$, the cage formed by the four j atoms is distorted and the molecular axis is located in the first well. The molecular c.m. is appreciably displaced from the site center. Then the excited molecule quickly jumps into the second well and pushes back its two NN j atoms of the $\gamma = 2$ well. These atoms tend to follow the molecule motion for $\tau \sim 4$ and the molecule then nearly stops up to $\tau = 6$. At $\tau \sim 8$, the molecular rotation starts and the molecule jumps into the third well, around $\tau = 10$. An energy transfer towards the c.m. motion of the molecule occurs which strongly displaces the location of the molecule with respect to its site. Then the molecule

goes back to the site center and tends to librate inside the $\gamma = 3$ well with a strong coupling with the vibrations of the j atoms.

When Γ/ω increases, the rotational motion tends to be more damped and the molecular axis cannot jump into the third well. The molecule remains in the $\gamma = 2$ well and librates in this well. The coupling of the libration with the vibrations of the j atoms is greater than with the theoretical value of the damping parameter. The details of the molecule and of the cage motions are presented in Fig. 7. Note the consistency between the kinetic energy behavior and the photographies of the trajectory.

2. Thermal conditions

An equivalent scheme has been studied when the CO molecule is in thermal equilibrium (at $T = 20$ K) with the surrounding crystal and for the same theoretical conditions $\Gamma/\omega = 0.16$ and $\Omega/\omega^2 = 0.024$. The three previous cases, $\theta = \theta_{\text{thermal}}$, $\theta = \theta_{\min}$, and $\theta = \theta_{\max}$ have been investigated. The results concerning the whole behavior are not very different. The main discrepancy concerns the rotational behavior of the molecule.

Figure 8 exhibits the kinetic energies associated to the primary system for a particular trajectory starting from the initial configuration with $\theta = \theta_{\max}$ and the other values given by the Monte Carlo procedure. The time behavior of the θ angle connected to the molecular rotation is also shown when $\theta = \theta_{\max}$ and $\theta = \theta_{\text{thermal}}$ for the P_1 configuration issued from the Monte Carlo sampling. One can see that, from $\theta_{\max}$, the molecule rotates inside the first well ($\gamma = 1$), then librates around $\theta = \pi/2$ (which corresponds to a minimum potential energy), and finally jumps back to the well $\gamma = 4$. The study of the same curve $\theta(\tau)$, when $\theta = \theta_{\text{thermal}}$, leads to the occurrence of two typical angular positions for the molecular axis. Indeed, the molecule remains confined in its origin well but librates first around $\theta = 77°$ and then around $\theta = 97°$ (located on each side of the equilibrium minimum $\theta = \pi/2$) before going back and making librations around this latter equilibrium value. If the matrix cage and the molecule c.m. were rigidly fixed, the libration would proceed around $\theta = \pi/2$. The occurrence of different angles $\theta = 77$

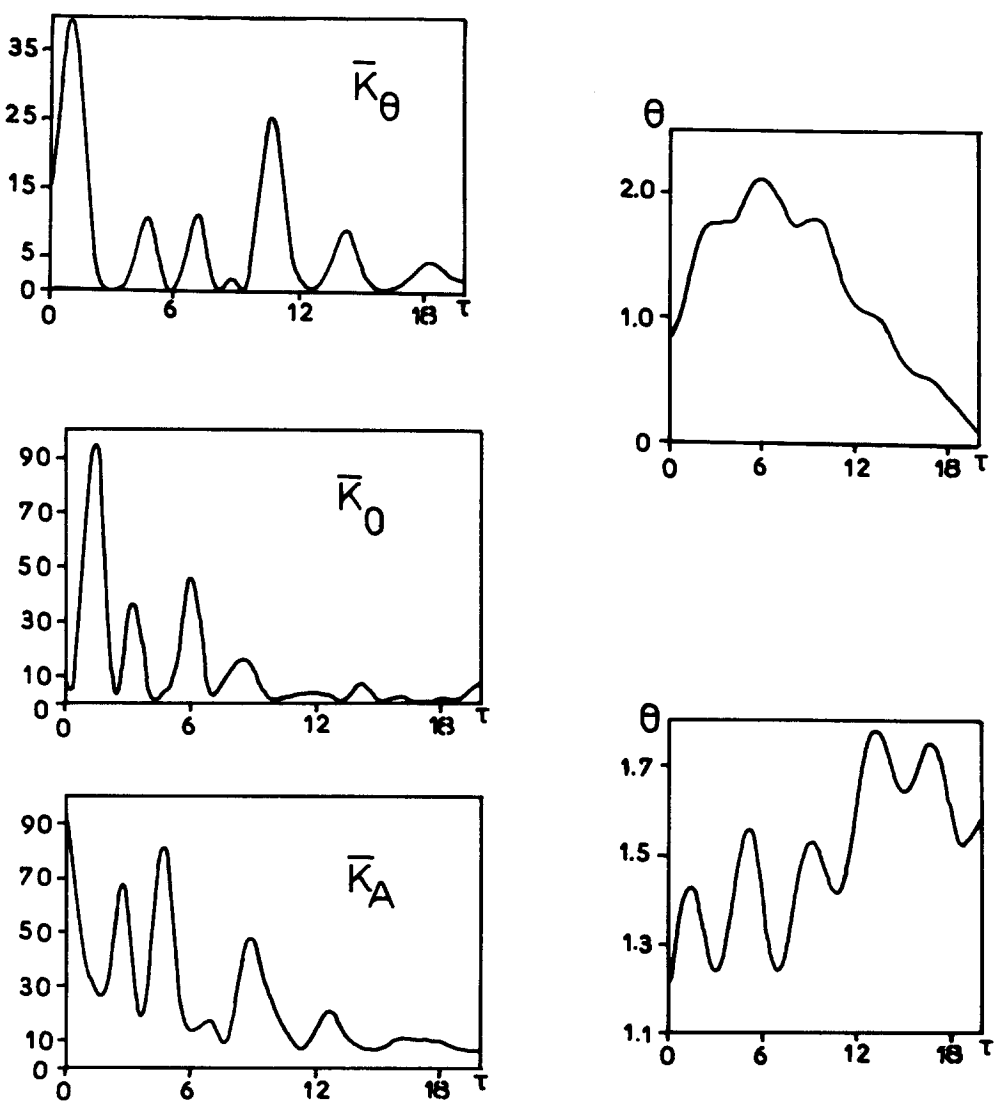

FIG. 8. Left: kinetic energies of the primary system (CO + four Ar) for a particular trajectory and $T^* = T = 20$ K. The initial configuration for the molecular axis corresponds to $\theta = \theta_{\max}$. Right: time behavior of the angle θ for two trajectories; upper: $\theta = \theta_{\max}$; lower: $\theta = \theta_{\text{thermal}}$.

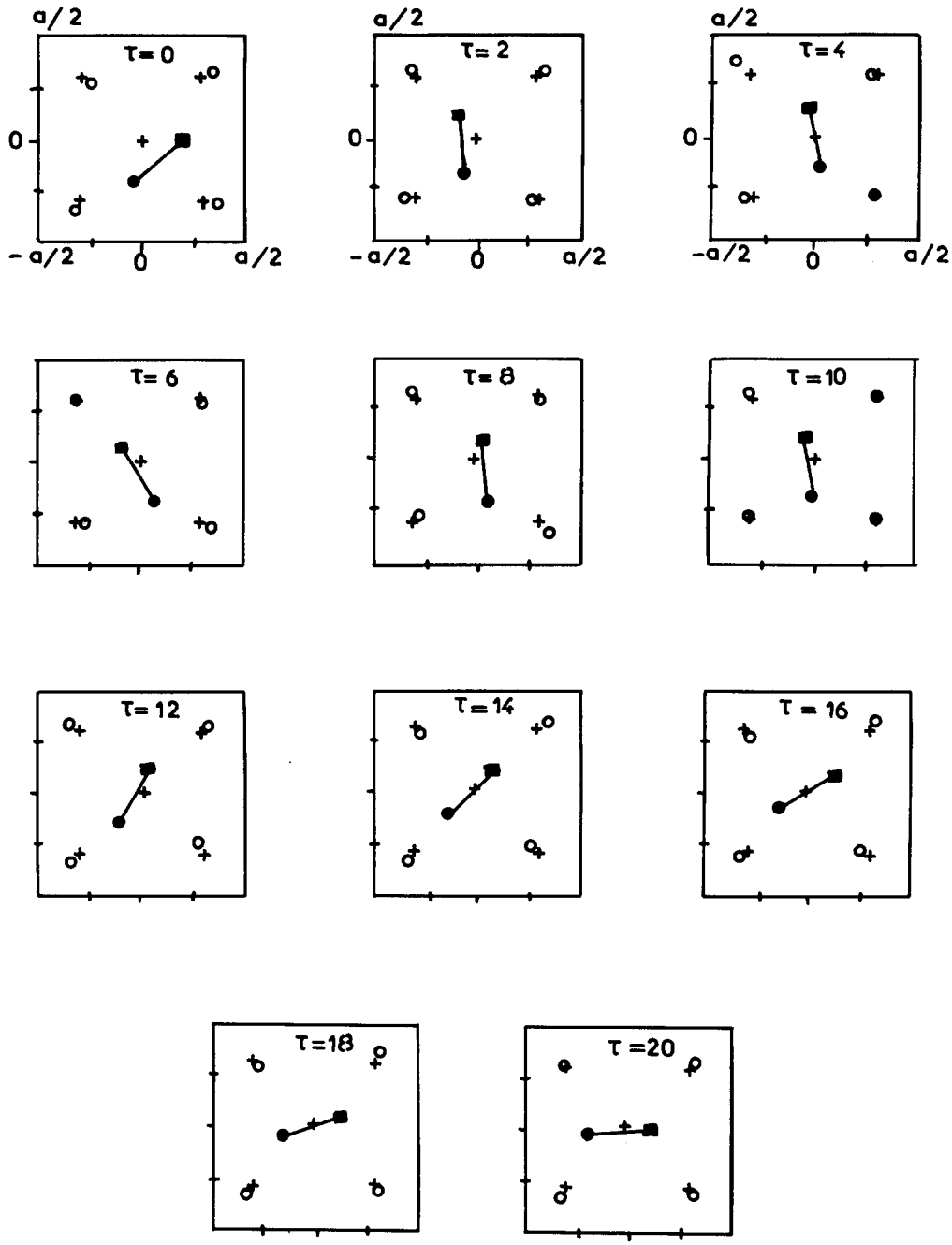

FIG. 9. Photographs of the instantaneous configuration of the primary system for a particular trajectory and $\theta = \theta_{max}$, $T^* = T = 20$ K, $\Gamma/\omega = 0.16$.

and 97 is a clear manifestation of the primary system distortion and of its simultaneous evolution when the molecule rotates. This corresponds to the pseudorotating cage motion qualitatively described by Manz.[4]

The matrix distortion is clearly exhibited in Fig. 9 which shows a particular trajectory of the primary system originating from the configuration $\theta = \theta_{max}$. When $\tau = 0$, the molecular c.m. and the four atoms are displaced from their site centers, since nothing has been required regarding the primary system configuration, except that $\theta = \theta_{max}$. As time proceeds, the molecular c.m. is strongly displaced, when the molecular axis rotates, towards the center of the first well. In this motion, for $2 \lesssim \tau \lesssim 4$, the molecule pushes back the atom belonging to the $\gamma = 1$ well, to which it faces. Then, for $4 \lesssim \tau \lesssim 8$, the molecule libration around this minimum equilibrium position is strongly coupled to the vibrations of the j atoms. In fact, the more displaced atom then transfers its energy to the molecule rotation in order to recover a lower energy corresponding to its site. This energy transfer is sufficient to induce a jump of the molecular axis in the well $\gamma = 4$, because, simultaneously, the two atoms which would *a priori* prevent such a jump are moved back. After the jump, the molecule librates in its new well ($\gamma = 4$) around $\theta = 0$.

V. CONCLUSION

To sum up, one can say that the rotational energy loss of a molecule trapped in a rare gas crystal is fast (over the

picosecond scale). The CO molecule, with a slightly anisotropic shape, seems to relax its rotational energy towards the bath in a direct way, when the viscous parameter Γ/ω is larger than 0.2. But if this parameter is smaller than the estimated value, the relaxation will proceed within the primary system. In contrast, the CH_3F molecule, more anisotropic, transfers its rotational energy for the same value of Γ/ω towards the primary system which thus plays the role of acceptor modes.

For an excitation of about 350 cm^{-1} the rotational motion is rapidly damped, since the possibility for the molecule to explore the four wells is very small. The molecule is strongly damped and makes angular oscillations which can reach a magnitude of about 25°–30° in the latter well. Such an orientational excitation corresponds, however, to a small part of the available vibrational energy ($\sim$20% for CO and $\sim$35% for CH_3F). Reversely, for a thermal excitation $T^* = T$, the molecule is generally trapped in a given well and makes librations strongly coupled to the motions of the surrounding atoms. It is nevertheless possible that an energy accumulation on the primary system and on the molecule c.m. is transferred back to the rotation and produces a jump to an adjacent well. The magnitude of the librational motions does not exceed 10°–15° in this case.

The autocorrelation function for the molecular axis decreases more rapidly for CO than for CH_3F and, consequently, the rotational transitions observed in infrared spectroscopy experiments are expected to have a larger width for the less anisotropic molecule.

For CO, the experimental results corroborate such a conclusion since the librational transition observed in the near infrared spectrum of CO trapped in argon is very broadened. This feature is conveniently interpreted by our model which leads to a linewidth of one to several wave numbers according to the temperature. The same conclusions concerning the position of the more intense librational transition and its broadening had been reached in a previous simplified model which considered the first matrix shell as a rigid system. The present results show that the distortion of the matrix is highly anisotropic and the matrix shell cannot therefore be considered as a whole undeformable system. Indeed, such a matrix deformation is able to induce molecule jumps! This study may also be considered as a classical quantitative interpretation of the pseudorotating cage model proposed by Manz.[4]

For CH_3F the experimental results are not so clear. Jones and Apkarian,[9] after many investigations on the high resolution infrared spectrum of the ν_3 mode of CH_3F, do not observe a librational residue. In contrast, Abouaf *et al.*[9] have observed small signals in the close neighborhood of the pure vibrational transition which they assigned to rotational residues. Given the present results which tend to show the strong coupling between the molecular rotation and the matrix motions and the occurrence of a librational peak narrower than the corresponding signal easily observed for CO trapped in the same matrix, it remains to be understood why the librational signal of CH_3F has never been unambiguously assigned!

To conclude, the present paper, although developing a classical point of view, can bring additional information as well on the energy relaxation as on the motions of a limited number of particles in a crystal. Even if quantum theories are now available for the CO molecule,[5] this study has the great advantage of giving a simple representation of an intricate problem. Note, however, that our calculations could be considerably improved[16] by first introducing a convenient description of the random forces and an effective temperature for the bath which incorporates the zero point energy of the system and allows low temperature (quantum) effects to be adequately accounted in this classical version. Second, one could also start with a model which connects the internuclear vibration of the molecule to the remaining degrees of freedom. These improvements are necessary for a quantitative analysis of the spectroscopic and time resolved experimental data but they require considerable and tedious numerical calculations.

APPENDIX: CALCULATION OF THE EQUILIBRIUM CONFIGURATION OF THE PRIMARY SYSTEM

Let us introduce $\hat{\mathbf{u}}' = \hat{\mathbf{d}} + \hat{\mathbf{u}}$ such that

$$\hat{F}_{u'} = -\nabla\hat{\mathscr{V}}(\hat{\mathbf{u}}') = 0, \quad \hat{\mathbf{u}}' \equiv \hat{\mathbf{d}}, \tag{A1}$$

where $\hat{\mathscr{V}}$ is the reduced potential defined in Eq. (6) of paper I. The calculation of $\hat{\mathbf{u}}'$ can be performed from the integration of the following equation of motion:

$$\ddot{\hat{\mathbf{u}}}' = -\nabla\hat{\mathscr{V}}(\hat{\mathbf{u}}') - \hat{\beta}'\dot{\hat{\mathbf{u}}}' \tag{A2}$$

over an infinite time:

$$\hat{\mathbf{u}}'(t \to \infty) \equiv \hat{\mathbf{d}}.$$

Such a value is β' independent, but in practice, the computational time of the numerical procedure will be faster if $\hat{\beta}'$ is conveniently chosen. The introduction of $\hat{\beta}'$ thus corresponds to an *artificial* mathematical process to fasten the computation of the equilibrium since $\hat{\beta}'$ tends to damp the motions of the atoms and to change it into a drift toward the final equilibrium.

Equation (A2) is nothing but Eq. (8), after substitution of $\hat{\mathbf{u}}$ by $\hat{\mathbf{u}}'$:

$$\ddot{\mathbf{u}}' = \hat{\mathbf{F}}_{u'} + \hat{\Lambda}_{u'}(0)(\hat{\mathbf{u}}' - \hat{\mathbf{d}}) - \hat{\beta}_{u'}\dot{\hat{\mathbf{u}}}' + \hat{N}_{u'} \tag{A3}$$

and taking

$$\begin{aligned} &\hat{\Lambda}_{u'}(0)(\hat{\mathbf{u}}' = \hat{\mathbf{d}}) = 0, \\ &\hat{N}'_{u} = 0, \\ &\hat{\beta}_{u'} \equiv \hat{\beta}'. \end{aligned} \tag{A4}$$

Equations (A4) are equivalent to the modifications given in items (i)–(iv) which are only specific of the equilibrium calculations.

[1] V. Delgado, J. Breton, and C. Girardet, J. Chem. Phys. **87**, 4802 (1987).
[2] S. W. Charles and K. O. Lee, Trans. Faraday Soc. **61**, 614 (1965); K. O. Lee, Can. J. Phys. **49**, 2018 (1971).
[3] K. Mirsky, Chem. Phys. **46**, 445 (1980); J. Manz and K. Mirsky, *ibid.* **46**, 457 (1980).
[4] J. Manz, J. Am. Chem. Soc. **102**, 1801 (1980).
[5] E. Blaisten-Barojas and M. Allavena, Int. J. Quantum Chem. **7**, 195 (1973); J. Phys. C **9**, 3121 (1976); I. L. Garzon and E. Blaisten-Barojas, J. Chem. Phys. **83**, 4311 (1985).

[6]F. Mauricio, S. Velasco, C. Girardet, and L. Galatry, J. Chem. Phys. **76**, 1624 (1982).
[7]H. Dubost, Chem. Phys. **12**, 139 (1976); H. Dubost and R. Charneau, *ibid.* **12**, 407 (1976); H. Dubost, A. Lecuyer, and R. Charneau, Chem. Phys. Lett. **66**, 191 (1979).
[8]C. Girardet and A. Lakhlifi (unpublished results).
[9]B. Gauthier-Roy, C. Alamichel, A. Lecuyer, and L. Abouaf-Marguin, J. Mol. Spectrosc. **88**, 72 (1981); L. H. Jones and B. I. S. Wanson, J. Chem. Phys. **76**, 1634 (1982); **77**, 6338 (1982); K. A. Apkarian and E. Weitz, *ibid.* **76**, 5796 (1982).
[10]L. Abouaf-Marguin, B. Gauthier-Roy, and F. Legay, Chem. Phys. **23**, 443 (1977); L. Young and C. B. Moore, J. Chem. Phys. **76**, 5869 (1982).
[11]A. Hardisson, C. Girardet, and L. Galatry, Chem. Phys. **92**, 319 (1985).
[12]J. W. Brady, J. D. Doll, and D. L. Thompson, J. Chem. Phys. **74**, 1026 (1981); I. Nodrbatcha, L. M. Raff, and D. L. Thompson, *ibid.* **81**, 3715 (1984); **82**, 1543 (1985).
[13]A. O. Caldeira and A. J. Legett, Phys. Rev. Lett. **46**, 211 (1981).
[14]P. G. Wolynes, Phys. Rev. Lett. **47**, 968 (1981).
[15]R. Meyer and R. R. Ernst, J. Chem. Phys. **86**, 784 (1987).
[16]M. Shugard, J. C. Tully, and A. Nitzan, J. Chem. Phys. **69**, 336 (1978); A. Nitzan and J. C. Tully, *ibid.* **78**, 3959 (1983), and references therein.
[17]A. Kitaigorodsky, in *Molecular Crystals and Molecules* (Academic, New York, 1973).